Hindawi Publishing Corporation
Indian Journal of Materials Science
Volume 2013, Article ID 718304, 7 pages
http://dx.doi.org/10.1155/2013/718304

Research Article

Electrical Conductivity Studies of Polyaniline Nanotubes Doped with Different Sulfonic Acids

Mohd. Khalid, Milton A. Tumelero, Iuri. S. Brandt, Vinicius C. Zoldan, Jose J. S. Acuña, and Andre A. Pasa

Laboratório de Filmes Finos e Superfícies, Departamento de Fisica, Universidade Federal de Santa Catarina, 88040-900 Florianopolis, Brazil

Correspondence should be addressed to Mohd. Khalid; mkansarister@gmail.com and Andre A. Pasa; andre.pasa@ufsc.br

Received 15 October 2013; Accepted 10 November 2013

Academic Editors: S. K. Dhara, S. K. Kulshreshtha, and V. Privman

Self-assembled polyaniline (PANI) nanotubes were prepared in the presence of three different sulfonic acids as dopant, namely, p-toluenesulfonic acid, camphorsulfonic acid, and tetrakis(4-sulfonatophenyl)porphyrin, by oxidative polymerization using ammonium peroxydisulfate as the oxidant. The morphology of the PANI nanotubes was determined by SEM and TEM and the electrical conductivity was measured as a function of temperature. The PANI nanotubes were also characterized by FTIR, XRD, UV-Vis, and cyclic voltammetry. We have found that the dopants had a noteworthy effect on the electrical conductivity whithout significant changes in the morphology of the PANI nanotubes.

1. Introduction

Polyaniline is a prototype conducting polymer; it is particularly attractive for electronic applications due to its facile synthesis, environmental stability, unique electronic properties, and simple acid/base doping/dedoping chemistry [1]. *In situ* polymerization is one of the most important methods developed so far to incorporate the dopant in polyaniline during synthesis. A great variety of organic and inorganic dopant acids can be used, such as hydrochloric, sulfuric, nitric, phosphoric, perchloric, acetic, formic, tartaric, camphorsulfonic, methylsulfonic, ethylsulfonic, and 4-toluenesulfonic acid. The size and amount of dopants play an important role in influencing the morphology of conducting polymers. Recently, we have demonstrated that the morphology of sulfonated porphyrin doped polyaniline can be changed from one-dimensional nanotube to three-dimensional cauliflower structure by simply changing the volume ratio of dopant to aniline [2]. In our earlier reported work, we have prepared conducting fibrous polyaniline: nylon-6,6 by stirring aniline and nylon-6,6 solution with the help of magnetic bar, as in this technique the conductivity of the fibrous material depends on the ratio of conducting polymer present in fibrous material [3, 4]. Zhang et al. have demonstrated that the polymeric acid has significant effect on the morphology and size of the polyaniline nanotubes [5]. Many techniques have been used to synthesize PANI nanostructure such as stirring [6–8], static placement, [9] sonication [10–12], and emulsion polymerization [13–16]. Particularly, conducting polymer nanotubes and nanofibers have received growing interest in recent years due to their unique properties and promising potential applications in nanodevices [17–21]. The investigation of nanostructured conducting polymers has great importance for both scientific and technological points of view.

In this work, we report the effect of dopants such as p-toluenesulfonic acid (TSA), camphorsulfonic acid (CSA), and tetrakis(4-sulfonatophenyl)porphyrin (TSPP) on the electrical conductivity of self-assembled PANI nanotubes. The obtained PANI nanotubes were characterized by measuring electrical conductivity, scanning electron microscopy (SEM), transmission electron microscopy (TEM), Fourier transform infrared spectroscopy (FTIR), UV-Vis spectroscopy (UV-Vis), X-ray diffraction (XRD), and cyclic voltammetry.

2. Experimental Detail

2.1. Chemicals. Aniline, camphorsulfonic acid, *p*-toluenesulfonic acid, ammonium peroxydisulfate ($(NH_4)_2S_2O_8$, APS), and N-methyl-2-pyrrolidone (NMP) were obtained

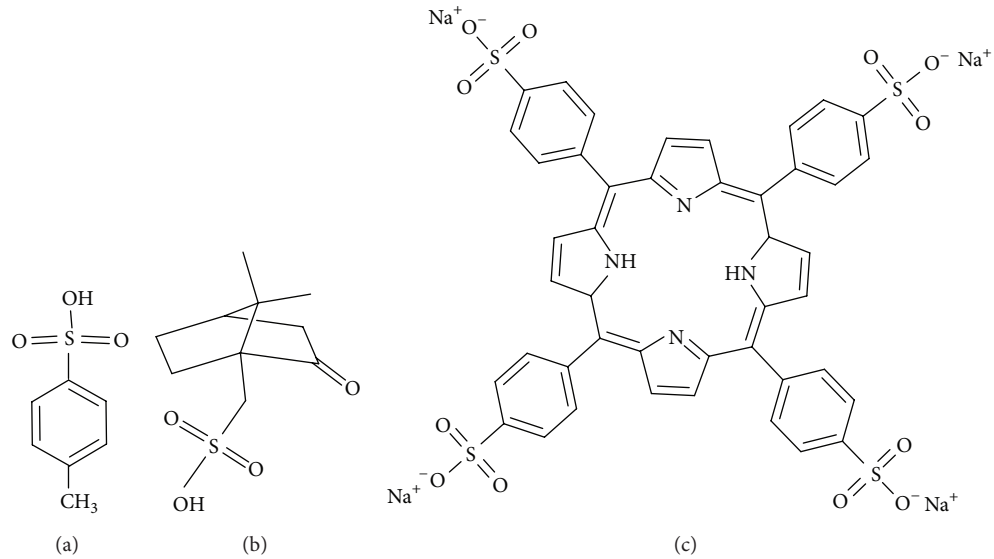

Figure 1: Molecular structure of (a) TSA, (b) CSA, and (c) TSPP.

from Synth Chem. Co., Brazil. Tetrakis(4-sulfonatophenyl) porphyrin was from Sigma Aldrich Co. Aniline was distilled twice before use. All solutions were prepared using Milli-Q grade water.

2.2. Synthesis. The preparation procedure for the PANI nanotubes was followed as described in our previous publication [2]. Solutions of 0.1 mL aniline (dissolved in 20 mL deionized water) and 20 mL sulfonic acids in question of 0.02 mL^{-1} TSA, 0.02 mL^{-1} CSA, or 0.0001 mL^{-1} TSPP were mixed under supersonic stirring for 10 min (the molecular structures of TSA, CSA, and TSPP are given in Figure 1). Then, precooled aqueous solution of ammonium peroxydisulfate (0.54 g in 40 mL deionized water) was rapidly mixed into the above reaction mixture. The mixture was left overnight in an ice bath without disturbing. These conditions were optimized to obtain high quantity of nanotubes. The product was filtered and washed with deionized water, methanol, and finally ether, and then dried in vacuum for 24 h to obtain a green-black PANI powder.

2.3. Characterization. The morphologies of the products were investigated with JEOL JSM-6701F field-emission scanning electron microscope (SEM) and JEOL JEM-1011 transmission electron microscope (TEM). The samples for SEM were mounted on aluminum stubs without sputter-coating of gold. Samples for TEM measurements were dispersed in ethanol and coated on copper microgrids with a carbon support film. Infrared spectra in the range 400–4000 cm^{-1} on sample pellets made with KBr were measured by means of an infrared spectrophotometer (Perkin Elmer Tensor 100). After dissolving 1-2 milligrams of the product (TSA-PANI, CSA-PANI, and TSPP-PANI) in 10 mL NMP and filtering, UV-visible spectra of the products were recorded from 300 to 1000 nm using Perkin Elmer 750 spectrophotometer. X-ray scattering of the samples was carried out on X-ray diffraction instrument (with CuK_α radiation). Electrical characterization of the doped polyanilines was performed by four-probe method, under collinear contact geometry on top of compressed pallet, as shown in the button-right inset of Figure 7(a). The data was collected at temperatures ranging from 100 to 300 K, in low vacuum ambient (~10^{-3} mbar). The electrical conductivity was determined from the conductance measurements multiplied by the geometrical factor. The four-probe method eliminates the influence of leads resistance or contact resistance, providing a better accuracy for measuring conductance. Samples were pelletized to a diameter of 13 mm and a thickness of 0.4 mm using a vacuum press at 8 MPa for 5 min.

2.4. Cyclic Voltammetry. The electrochemical response of the material was determined using an Autolab PGSTAT-30 electrochemical workstation. Each sample was first dispersed in $CHCl_3$ and the dispersion was dropped onto a gold plate ($1 \times 2\,cm^2$) working electrode which was allowed to dry at room temperature. The cell was filled with 0.1 M H_2SO_4 and purged with N_2 for approximately 15 min. Following this, N_2 was allowed to flow over the solution to prevent O_2 from reentering the cell for the remaining experiment. Cyclic voltammograms were recorded in the potential range from −0.5 V to 1.0 V at scan rates of 60 mV s^{-1}, using a saturated calomel as reference electrode and a Pt foil as counter electrode.

3. Results and Discussion

3.1. Morphology. SEM images (Figures 2(a)–2(c)) show the tubular morphology of the resulting PANI in the presence of TSA, CSA, and TSPP as the depots. TEM images (Figures 2(a′)–2(c′)) prove the hollow-tube morphology of the PANI. The SEM images point up that the molecular

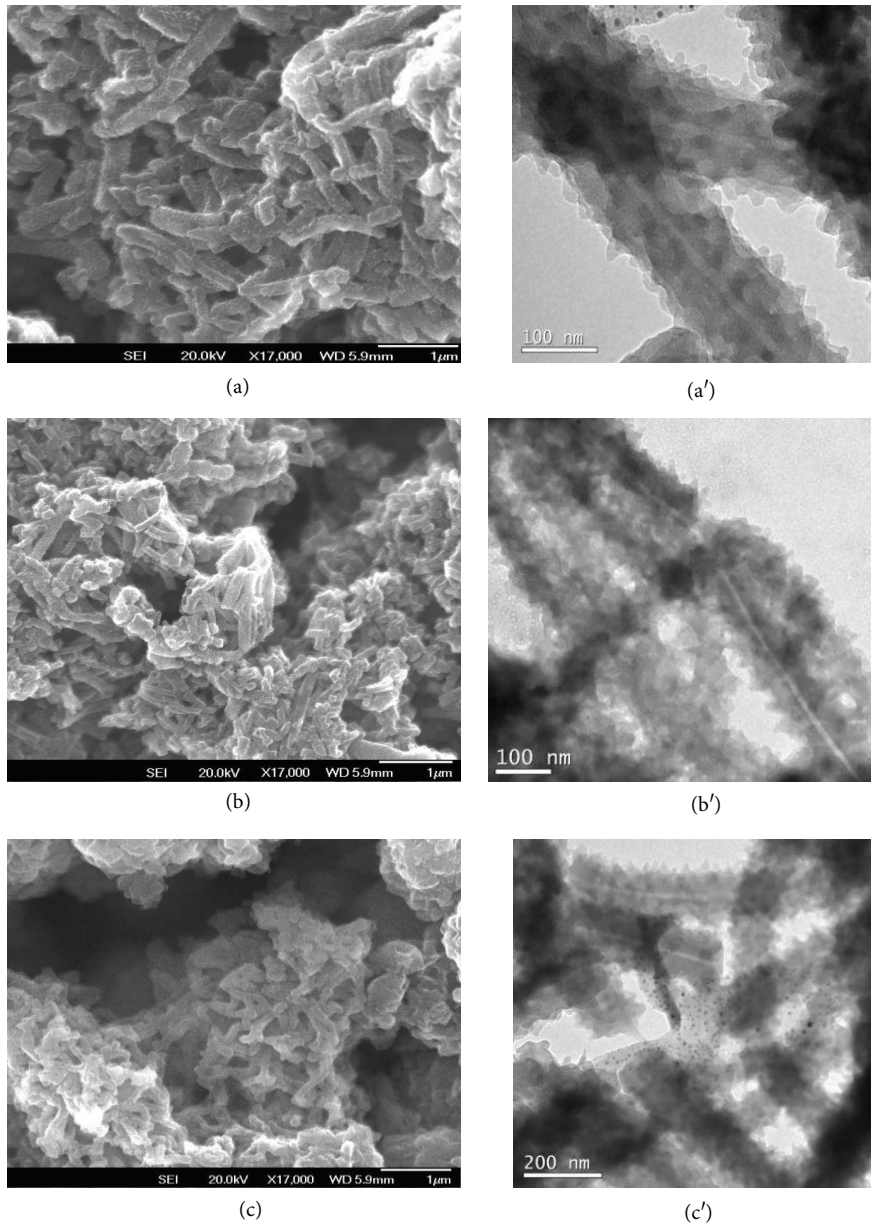

Figure 2: SEM and TEM images of PANI nanotubes obtained from solutions that contained different sulfonic acids: (a) TSA, (b) CSA, and (c) TSPP.

structures of dopants had an effect on the length and diameter of the nanotubes, with less effect on the surface morphology. The TSA doped PANI nanotubes have bigger diameter of about 140 nm as compared to CSA doped of about 100 nm and TSPP doped of about 120 nm. These differences could be due to the difference in molecular structure of the dopants. During polymerization, aniline cation-radical surfactant could be aggregated in different sizes and types of micelles by introducing dopant counterions [22].

3.2. FTIR. Figure 3 shows FTIR spectra for the PANI nanotubes doped with different organic acids (CSA-PANI, TSA-PANI, and TSPP-PANI). The spectra of nanotubes are in agreement with previous reported data for PANI [23], confirming that the nanotubes are in doped state. For example, the nanotubes show the characteristic peaks of PANI at 1600 and 1497 cm^{-1} (quinoid and benzenoid rings, resp.), 1301 cm^{-1} (C–N stretching), 1172 cm^{-1} (C=N stretching), and 823 cm^{-1} (1,4-substituted phenyl ring stretching), which are identical to the emeraldine salt form of PANI [24]. A peak at 1246 cm^{-1}, ascribed to the $C–N^+$ stretching vibration in the polaron structure, is also observed, indicating that the PANI is in a doped state [25]. The peaks at 1080 cm^{-1} can be assigned to the asymmetric and symmetric O=S=O stretching vibrations, respectively, denoting the existence of SO_3^- groups [26, 27]. The S–O stretching peak is at 750 cm^{-1},

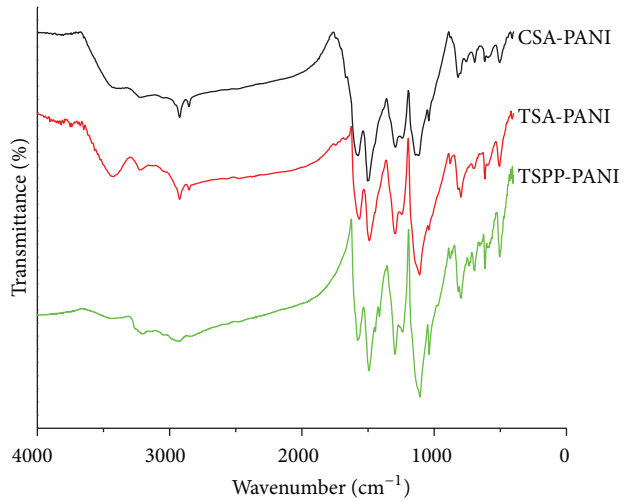

Figure 3: FTIR spectra of CSA-PANI, TSA-PANI, and TSPP-PANI nanotubes.

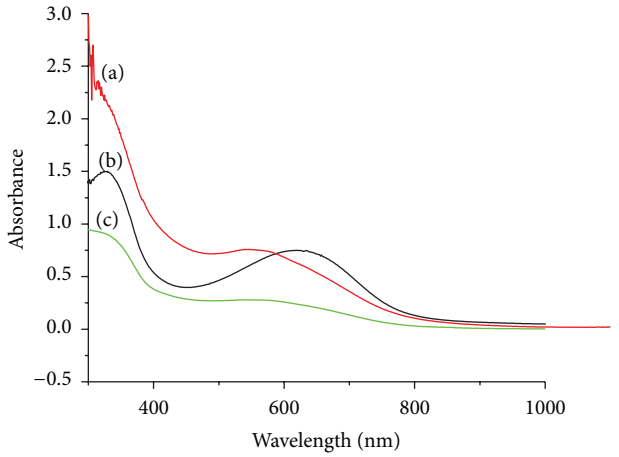

Figure 4: UV-visible absorption spectra of PANI nanotubes dissolved in N-methyl-2-pyrrolidone. (a) TSPP doped PANI nanotubes, (b) TSA doped PANI nanotubes, and (c) CSA doped PANI nanotubes.

while the peak at 630 cm^{-1} represents the C–S stretching vibration. The absorption peaks at 1080, 750, and 630 cm^{-1} in the FTIR spectra for all samples are consistent with the presence of the $-SO_3^-$ group attached to the aromatic rings [28].

3.3. UV-Vis. Figure 4 shows the UV-Vis spectra of doped PANI nanotubes dispersed in N-methyl-2-pyrrolidone by using ultrasonic bath. The UV-Vis absorption patterns of the nanotubes obtained are consistent with the previously reported work [29–31]. The two absorption peaks for all three samples are indicating that the samples are in doped state, and the second peak nearly about 600 nm for all three samples assigns the polaron band [32]. The peaks at 580 nm for TSPP-PANI and 600 nm for CSA-PANI are blue shifted in comparison of the peak at 640 for TSA-PANI. The difference

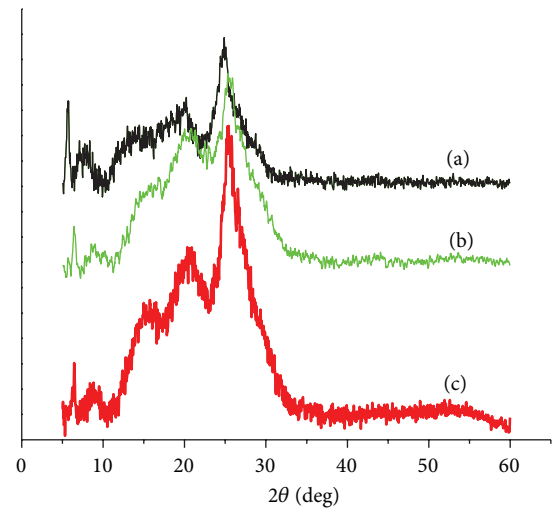

Figure 5: XRD scattering pattern of PANI nanotubes. (a) TSPP doped, (b) CSA doped, and (c) TSA doped.

in the band shifting might be the reason of the molecular interaction of dopants with imine nitrogen of PANI.

3.4. XRD. Figure 5 shows the XRD patterns of PANI nanotubes with the different sulfonic acids. The present X-ray scattering patterns of nanotubes, showing five peaks centered at $2\theta = 6.3^\circ$, 8.1°, 15°, 20°, and 25°. The sharp peak centered at $2\theta = 6.3^\circ$ assigned to the periodic distance between the dopant and the N atom on adjacent main chains [33]. The latter two bands may be attributed to the repeat unit of the polyemeraldine chain ($2\theta = 6.3^\circ$) [34] and the periodicity parallel to the polymer chains of PANI ($2\theta = 8.1^\circ$ and 15°) [35]. As one can see, two sharp broad bands centered at $2\theta = 20^\circ$, 25° compared to the CSA and TSPP doped PANI nanotubes are observed in the pattern of TSA doped PANI nanotubes, which indicates that the TSA doped nanotubes are more crystalline than those of CSA and TSPP doped nanotubes, which may also be the reason of higher conductivity of TSA doped PANI nanotubes.

3.5. Cyclic Voltammetry. From the cyclic voltammograms represented in Figure 6, we can observe that the oxidation and reduction potentials are different for each dopant acid doped PANI nanotubes. This fact is attributed to the electrostatic interaction of the dopant with the chemically flexible –NH group of the polymer [36]. Cyclic voltammogram of TSA and CSA doped PANI nanotubes exhibits one set of redox peaks in comparison to TSPP doped PANI nanotubes. This could be attributed to the fact that the decrease of the charge delocalization and difficulties in ion movement inside the TSPP doped PANI chain is caused by the presence of the substituent bulky group of porphyrin. This may be the reason of lower conductivity of TSPP doped PANI nanotubes than TSA and CSA doped PANI nanotubes.

3.6. Electrical Conductivity. The $I \times V$ curves of TSA-PANI samples are shown in Figure 7(a). The linear trend

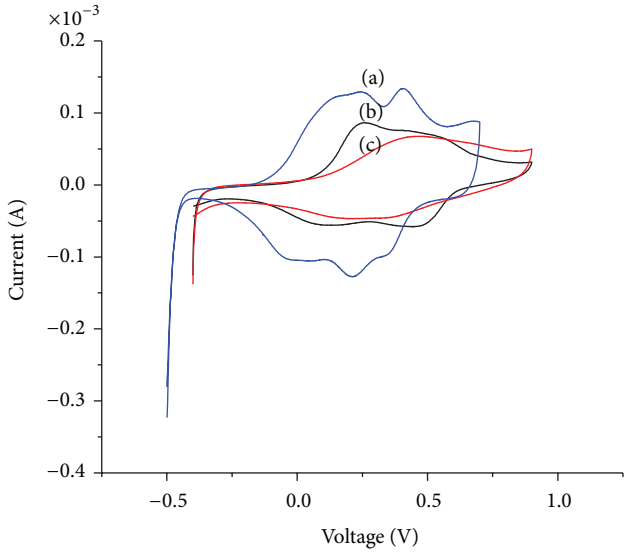

FIGURE 6: Cyclic voltammetric response of polyaniline nanotubes in 1 M of H_2SO_4 solution at a scan rate of 60 mV/s. (a) TSPP doped, (b) TSA doped, and (c) CSA doped.

was observed for all samples measured in this work and allowed us to calculate the conductivity from the slope of the straight lines. The electrical conductivities are shown in Figure 7(b) as a function of temperature. All samples showed a clear reduction of the conductivity by lowering the temperature, that is, less than one order of magnitude for TSA and CSA doped PANI nanotubes and about two orders of magnitude for TSPP doped PANI nanotubes. The values for the conductivity at room temperature (RT) are 320 S/m for TSA-PANI, 15 S/m for CSA-PANI, and 3×10^{-6} S/m for TSPP-PANI. TSA and CSA-PANI are, at least, seven times more conductive than undoped (~10^{-7} S/m) PANI [37], making these materials suitable for electrical application. TSA and CSA-PANI conductivities, at RT, are in good agreement with those reported elsewhere [38, 39]. The dependency of the conductivity with temperature follows an activation behavior that can be described by the exponential equation

$$\sigma = \sigma_0 e^{-(T_0/T)^{1/2}}, \quad (1)$$

where σ_0 is a constant and T_0 is the Mott characteristic temperature of the system. The parameter T_0 is proportional to the inverse of localization length, assuming elevated values for highly localized polymers. This model is frequently applied to sulfonated doped polymers [40, 41] and known as quasi-1D Variable Range Hopping (VRH) [42]. By fitting the data with (1), as shown in Figure 7(b), by the continuous line, we determined the characteristic temperature T_0 for the three doped polymers. The obtained values were 835, 2310, and 3×10^4 K for TSA-, CSA-, and TSPP-PANI, respectively. For the most conductive ones, TSA and CSA-PANI, the model described adequately the whole interval of temperature, and, for TSPP-PANI, the fitting works properly at more elevated temperatures as already observed in our previous reported work [2]. The characteristic temperature obtained for TSPP-PANI is close to the values for low conductivity undoped

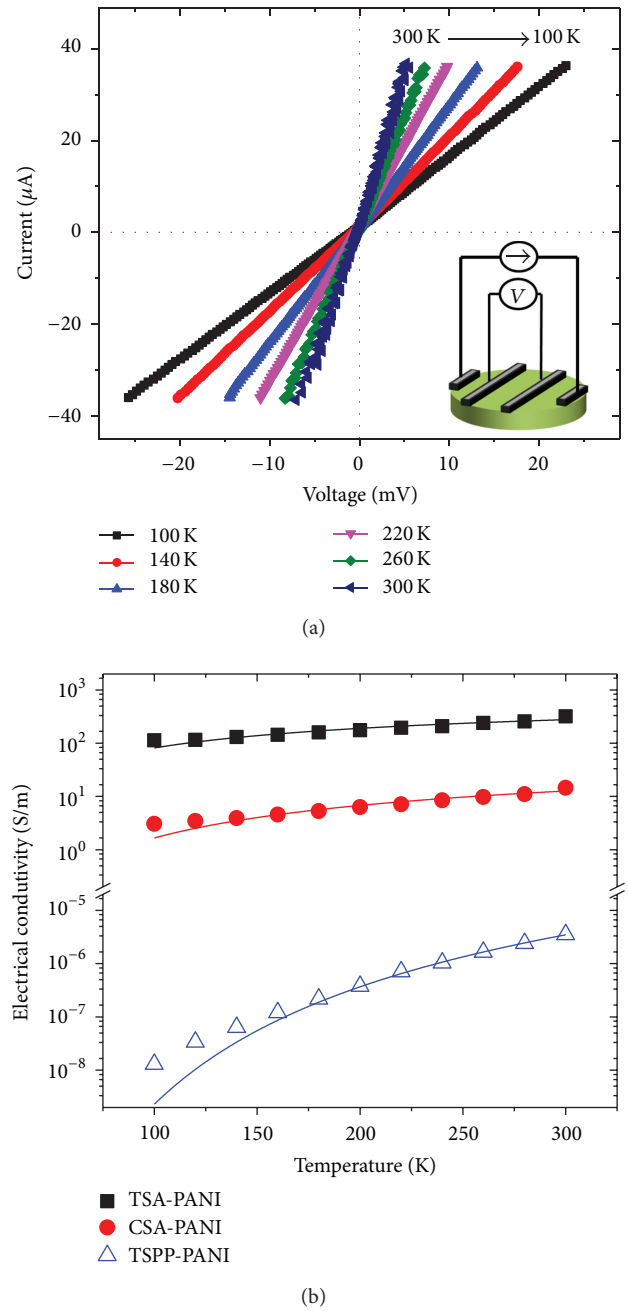

FIGURE 7: (a) $I \times V$ curves at different temperatures, obtained by four-probe measurements, for TSA-PANI sample. The inset illustrates the sample contacts and the electrical measurement. (b) Conductivity of the three doped samples as a function of the temperature.

PANI and PANI blends [43, 44] and those for TSA and CSA doping are well comparable with those found in [40]. The values of T_0 suggest that the disorder is much higher in TSPP doped PANI nanotubes than CSA and TSA doped PANI nanotubes this is good agreement with the XRD data. This is also in agreement with the fact that TSPP molecules are relatively large in size and compact which could induce a higher structural disorder and consequently a decrease in the mobility of the carriers.

4. Conclusions

Polyaniline nanotubes have been synthesized in the presence of three different sulfonic acid dopants (TSA, CSA, and TSPP). It was observed that the surface morphology does not change significantly, although the size (length and diameter) of the obtained PANI nanotubes was affected by the molecular structure of the dopants. TSA doped PANI nanotubes have higher electrical conductivity than CSA and TSPP doped PANI nanotubes. The materials were well characterized by electrical conductivity, SEM, TEM, FTIR, UV-Vis, XRD, and cyclic voltammetry. On the basis of the described above results, the PANI nanotubes could be important materials for technological points of view in terms of morphology, size, and electrical conductivity.

Acknowledgments

One of authors (Mohd. Khalid) would like to place in record his special thanks to the REUNI/CAPES and CAPES/PNPD, Government of Brazil, for providing the postdoctoral fellowship to carry out part of the research work in the Physics Department of UFSC, Florianopolis. The authors also thank Professor A. Neves (LBC/UFSC, Brazil) for providing FTIR and hydraulic pressure machine facilities and the Brazilian agencies CNPQ, FINEP, and FAPESC.

References

[1] D. Li, J. X. Huang, and R. B. Kaner, "Polyaniline nanofibers: a unique polymer nanostructure for versatile applications," *Accounts of Chemical Research*, vol. 42, pp. 135–145, 2009.

[2] M. Khalid, J. J. S. Acuña, M. A. Tumelero, J. A. Fischer, V. Zoldan, and A. A. Pasa, "Sulfonated porphyrin doped polyaniline nanotubes and nanofibers: synthesis and characterization," *Journal of Materials Chemistry*, vol. 22, pp. 11340–11346, 2012.

[3] M. Khalid and F. Mohammad, "Preparation, FTIR spectroscopic characterization and isothermal stability of differently doped fibrous conducting polymers based on polyaniline and nylon-6,6," *Synthetic Metals*, vol. 159, pp. 119–122, 2009.

[4] A. A. Khan and M. Khalid, "Preparation, FTIR spectroscopic characterization and isothermal stability of differently doped conductive fibers based on polyaniline and polyacrylonitrile," *Synthetic Metals*, vol. 160, no. 7-8, pp. 708–712, 2010.

[5] L. Zhang, H. Peng, J. Sui, P. A. Kilmartin, and J. Travas-Sejdic, "Polyaniline nanotubes doped with polymeric acids," *Current Applied Physics*, vol. 8, no. 3-4, pp. 312–315, 2008.

[6] Q. Yao, L. D. Chen, W. Q. Zhang, S. C. Liufu, and X. H. Chen, "Enhanced thermoelectric performance of single-walled carbon nanotubes/polyaniline hybrid nanocomposites," *ACS Nano*, vol. 4, no. 4, pp. 2445–2451, 2010.

[7] R. Sainz, W. R. Small, N. A. Young et al., "Synthesis and properties of optically active polyaniline carbon nanotube composites," *Macromolecules*, vol. 39, no. 21, pp. 7324–7332, 2006.

[8] X. T. Zhang, W. H. Song, P. J. F. Harris, G. R. Mitchell, T. T. T. Bui, and A. F. Drake, "Chiral polymer-carbon-nanotube composite nanofibers," *Advanced Materials*, vol. 19, no. 8, pp. 1079–1083, 2007.

[9] Y. Zhou, Z.-Y. Qin, L. Li et al., "Polyaniline/multi-walled carbon nanotube composites with core-shell structures as supercapacitor electrode materials," *Electrochimica Acta*, vol. 55, no. 12, pp. 3904–3908, 2010.

[10] G. M. Spinks, V. Mottaghitalab, M. Bahrami-Samani, P. G. Whitten, and G. G. Wallace, "Carbon-nanotube-reinforced polyaniline fibers for high-strength artificial muscles," *Advanced Materials*, vol. 18, no. 5, pp. 637–640, 2006.

[11] A. L. Cabezas, Z. B. Zhang, L. R. Zheng, and S. L. Zhang, "Morphological development of nanofibrillar composites of polyaniline and carbon nanotubes," *Synthetic Metals*, vol. 160, pp. 664–668, 2010.

[12] J.-Q. Dong and Q. J. Shen, "Enhancement in solubility and conductivity of polyaniline with lignosulfonate modified carbon nanotube," *Journal of Polymer Science B*, vol. 47, no. 20, pp. 2036–2046, 2009.

[13] P. Jimenez, W. K. Maser, P. Castell, M. T. Martínez, and A. M. Benito, "Nanofibrilar polyaniline: direct route to Carbon nanotube water dispersions of high concentration," *Macromolecular Rapid Communications*, vol. 30, pp. 418–422, 2009.

[14] P. Jimenez, P. Castell, R. Sainz et al., "Carbon nanotube effect on polyaniline morphology in water dispersible composites," *The Journal of Physical Chemistry B*, vol. 114, pp. 1579–1585, 2010.

[15] R. Sainz, A. M. Benito, M. T. Martínez et al., "Soluble self-aligned carbon nanotube/polyaniline composites," *Advanced Materials*, vol. 17, no. 3, pp. 278–281, 2005.

[16] M. Ginic-Markovic, J. G. Matisons, R. Cervini, G. P. Simon, and P. M. Fredericks, "Synthesis of new polyaniline/nanotube composites using ultrasonically initiated emulsion polymerization," *Chemistry of Materials*, vol. 18, no. 26, pp. 6258–6265, 2006.

[17] D. Normile, "Nanotubes generate full-color displays," *Science*, vol. 286, no. 5447, pp. 2056–2057, 1999.

[18] J. Kong, N. R. Franklin, C. W. Zhou et al., "Nanotube molecular wires as chemical sensors," *Science*, vol. 287, no. 5453, pp. 622–625, 2000.

[19] C. R. Martin, "Nanomaterials: a membrane-based synthetic approach," *Science*, vol. 266, no. 5193, pp. 1961–1966, 1994.

[20] J. Huang and M. X. Wan, "In situ doping polymerization of polyaniline microtubules in the presence of β-naphthalenesulfonic acid," *Journal of Polymer Science A*, vol. 37, no. 2, pp. 151–157, 1999.

[21] L. Zhang, H. Peng, P. A. Kilmartin, C. Soeller, and J. Travas-Sejdic, "Polymeric acid doped polyaniline nanotubes for oligonucleotide sensors," *Electroanalysis*, vol. 19, no. 7-8, pp. 870–875, 2007.

[22] Z. Zhang, Z. Wei, and M. Wan, "Nanostructures of polyaniline doped with inorganic acids," *Macromolecules*, vol. 35, no. 15, pp. 5937–5942, 2002.

[23] J.-C. Chiang and A. G. MacDiarmid, "'Polyaniline': protonic acid doping of the emeraldine form to the metallic regime," *Synthetic Metals*, vol. 13, no. 1–3, pp. 193–205, 1986.

[24] S.-A. Chen and H.-T. Lee, "Structure and properties of poly(acrylic acid)-doped polyaniline," *Macromolecules*, vol. 28, no. 8, pp. 2858–2866, 1995.

[25] M. Avram and G. D. Mateescu, *Infrared Spectroscopy: Applications in Organic Chemistry*, chapter 4, Wiley-Interscience, New York, NY, USA, 1972.

[26] M. Trchova, I. Sedenkova, E. N. Konyushenko, J. Stejskal, P. Holler, and G. C. Marjanovic, "Evolution of polyaniline nanotubes: the oxidation of Aniline in water," *The Journal of Physical Chemistry B*, vol. 110, pp. 9461–9468, 2006.

[27] E. C. Venancio, P.-C. Wang, and A. G. MacDiarmid, "The azanes: a class of material incorporating nano/micro self-assembled hollow spheres obtained by aqueous oxidative polymerization of aniline," *Synthetic Metals*, vol. 156, no. 5-6, pp. 357–369, 2006.

[28] A. J. Epstein, J. Joo, R. S. Kohlman et al., "Inhomogeneous disorder and the modified Drude metallic state of conducting polymers," *Synthetic Metals*, vol. 65, no. 2-3, pp. 149–157, 1994.

[29] R. S. Kohlman, J. Joo, Y. G. Min, A. G. MacDiarmid, and A. J. Epstein, "Crossover in electrical frequency response through an insulator-metal transition," *Physical Review Letters*, vol. 77, no. 13, pp. 2766–2769, 1996.

[30] J. G. Masters, Y. Sun, A. G. MacDiarmid, and A. J. Epstein, "Polyaniline: allowed oxidation states," *Synthetic Metals*, vol. 41, no. 1-2, pp. 715–718, 1991.

[31] Y. Xia, J. M. Wiesinger, A. G. MacDiarmid, and A. J. Epstein, "Camphorsulfonic acid fully doped polyaniline emeraldine salt: conformations in different solvents studied by an ultraviolet/visible/ near-infrared spectroscopic method," *Chemistry of Materials*, vol. 7, no. 3, pp. 443–445, 1995.

[32] B. J. Kim, S. G. Oh, M. G. Han, and S. S. Im, "Preparation of polyaniline nanoparticles in micellar solutions as polymerization medium," *Langmure*, vol. 16, pp. 5841–5845, 2000.

[33] M. Harada and M. Adachi, "Surfactant-mediated fabrication of Silica nanotubes," *Advanced Materials*, vol. 12, pp. 839–841, 2000.

[34] R. H. Baughman, J. F. Wolf, H. Echardt, and L. W. Schaklette, "The structure of a novel polymeric metal: acceptor-doped polyaniline," *Synthetic Metals*, vol. 25, pp. 121–137, 1998.

[35] J. P. Pouget, M. E. Józefowicz, A. J. Epstein, X. Tang, and A. G. MacDiarmid, "X-ray structure of polyaniline," *Macromolecules*, vol. 24, no. 3, pp. 779–789, 1991.

[36] M. Wan and J. Li, "Microtubules of polyaniline doped with HCl and HBF_4," *Journal of Polymer Science A*, vol. 37, pp. 4605–4609, 1999.

[37] V. I. Krinichnyi, S. D. Chemerisov, and Y. S. Lebedev, "EPR and charge-transport studies of polyaniline," *Physical Review B*, vol. 55, no. 24, pp. 16233–16244, 1997.

[38] J. Joo, H. G. Song, Y. C. Chung et al., "The effects of Dopant and solvent on charge transport of Doped polyanilines," *Journal of the Korean Physical Society*, vol. 30, pp. 230–236, 1997.

[39] J. Stejskal, I. Sapurina, M. Trchova, J. Prokes, I. Krivka, and E. Tobolkova, "Solid-state protonation and electrical conductivity of polyaniline," *Macromolecules*, vol. 31, no. 7, pp. 2218–2222, 1998.

[40] W. Lee, G. Du, S. M. Long et al., "Charge transport properties of fully-sulfonated polyaniline," *Synthetic Metals*, vol. 84, no. 1–3, pp. 807–808, 1997.

[41] Z. H. Wang, C. Li, E. M. Scherr, A. G. MacDiarmid, and A. J. Epstein, "Three dimensionality of "metallic" states in conducting polymers: polyaniline," *Physical Review Letters*, vol. 66, no. 13, pp. 1745–1748, 1991.

[42] K. P. Nazeer, S. A. Jacob, M. Thamilselvan, D. Mangalaraj, S. K. Narayandass, and J. Yi, "Space-charge limited conduction in polyaniline films," *Polymer International*, vol. 53, no. 7, pp. 898–902, 2004.

[43] B. Sanjai, A. Raghunathan, T. S. Natarajan et al., "Charge transport and magnetic properties in polyaniline doped with methane sulphonic acid and polyaniline-polyurethane blend," *Physical Review B*, vol. 55, no. 16, pp. 10734–10744, 1997.

[44] S. Kim and I. J. Chung, "Annealing effect on the electrochemical property of polyaniline complexed with various acids," *Synthetic Metals*, vol. 97, no. 2, pp. 127–133, 1998.